J Fluoresc (2007) 17:649–654
DOI 10.1007/s10895-006-0073-0

ORIGINAL PAPER

Monitoring Pyrene Excimers in Lactose Permease Liposomes: Revealing the Presence of Phosphatidylglycerol in Proximity to an Integral Membrane Protein

Laura Picas · Sandra Merino-Montero · Antoni Morros · Jordi Hernández-Borrell · M. Teresa Montero

Received: 13 October 2005 / Accepted: 23 January 2006 / Published online: 23 June 2006

Abstract In this study, we examined the annular lipid composition of the transmembrane protein lactose permease (LacY) from *Escherichia coli*. LacY was reconstituted into 1-Palmitoyl-2-Oleoyl-*sn*-Glycero-3-Phosphoethanolamine (POPE) and 1-Palmitoyl-2-Oleoyl-*sn*-Glycero-3-3-[Phospho-*rac*-(1-glycerol)] (POPG) and labeled with 1-hexadecanoyl-2-(1-pyrenedecanoyl)-*sn*-Glycero-3-phosphoglycerol (PPDPG) at a 3:0.99:0.01 molar ratio. Pyrene excimer formation was monitored by exciting a single tryptophan mutant of the protein (T320W). The results suggest that POPG remains segregated in the vicinity of the protein, most likely forming part of the annular composition. The possible involvement of POPG in hydrogen binding with the protein, as well as the molecular mechanism of LacY, is also discussed in the context of the proteomic network theory.

Keywords Lactose permease · Proteoliposomes · Pyrene excimer formation · Tryptophan · Energy transfer

L. Picas · S. Merino-Montero · J. Hernández-Borrell · M. T. Montero (✉)
Departament de Fisicoquímica, Facultat de Farmàcia, Universitat de Barcelona, 08028 Barcelona, Spain
e-mail: teremontero@ub.edu

A. Morros
Unitat de Biofísica, Departament de Bioquímica i Biología Molecular, Facultat de Medicina, Universitat Autònoma de Barcelona, 08193 Bellaterra, Barcelona, Spain

S. Merino-Montero · J. Hernández-Borrell · M. T. Montero
Centre de Bioelectrònica i Nanobiociència (CBEN), Parc Científic de Barcelona, 08028 Barcelona, Spain

Introduction

The lactose permease (LacY) of *Escherichia coli*, which is encoded by the *lac y* gene, the second structural gene in the *lac* operon, is an integral membrane protein that catalyzes the coupled stoichiometric translocation of β-galactosides and H^+ across the cytoplasmic membrane. LacY is one of the most studied cytoplasmic membrane proteins and is often used as a paradigm for those secondary transport proteins that couple the energy stored in an electrochemical ion gradient to a concentration gradient. The primary mechanism underlying LacY [1] was determined after analyzing the data compiled from a large variety of biophysical techniques [2], and was confirmed by X-ray diffraction of LacY crystals obtained after considerable effort [3]. Figure 1 displays the three-dimensional (3D) model of LacY rendered by using the program Protein Explorer [4]. LacY consists of 12 transmembrane α-helices, crossing the membrane in a zig-zag fashion, which are connected by 11 relatively hydrophilic, periplasmic, and cytoplasmic loops, with both amino and carboxyl termini on the cytoplasmic surface.

The physiological activity of transmembrane proteins may be influenced by, or be dependent upon, the physical properties of neighboring phospholipids [5]. While the matrices formed with neutral phospholipids have been used to reconstitute LacY (i.e., to obtain surface planar proteolipid sheets [6] and two-dimensional crystals [7,8]), the protein is only functional when reconstituted in native *Escherichia coli* extract membranes [9–14] or binary mixtures of phosphatidylglycerol (PG) and phosphatidylethanolamine (PE) [15–17]. The presence of phosphatidylethanolamine is a requirement for the *in vivo* function [18] and correct folding of LacY [19]. On the other hand, by using pyrene derivatives of phospholipids [20], the integration of LacY into liposomes

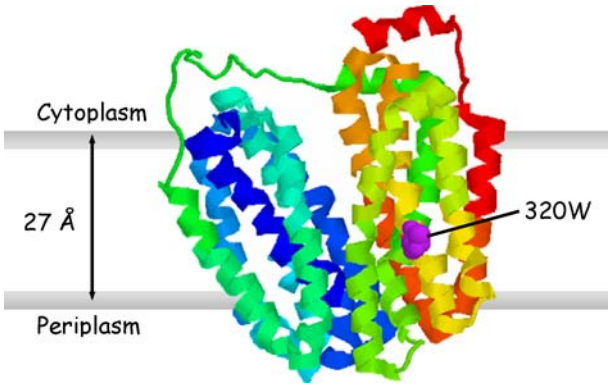

Fig. 1 The lactose permease of *Escherichia coli* adapted from reference 3, showing the position 320 in helix X. The original residue of threonine (T) has been replaced by tryptophan (W)

has been shown to induce the segregation of PG-forming microdomains. There remains, however, an apparent contradiction between the requirement of PE for LacY *in vivo* function, as well as the formation of PE nanometer domains, and the protein clusters we have visualized by means of atomic force microscopy (AFM) [21]. Therefore, it is necessary to explore the composition of the neighboring phospholipids, particularly the boundary or annular phospholipids, of Lac Y. The experiments presented in this paper were designed to investigate the presence of PG within the shell of adjacent boundary lipids (annular lipids) [22] by probing the transference of energy between a single-tryptophan mutant of LacY (T320W)[1] and a pyrene-labeled PG (1-hexadecanoyl-2-(1-pyrenedecanoyl)-*sn*-Glycero-3-phosphoglycerol (PPDPG)). These fluorescence measurements were complemented by two techniques: AFM and differential scanning calorimetry (DSC).

Materials and methods

Materials

N-dodecyl-β-D-maltoside (DDM) was purchased from Sigma Chemical Co. (St. Louis, MO, USA). 1-Palmitoyl-2-Oleoyl-*sn*-Glycero-3-Phosphoethanolamine (POPE), and 1-Palmitoyl-2-Oleoyl-*sn*-Glycero-3-[Phospho-*rac*-(1-glycerol)] (Sodium Salt) (POPG) were purchased from Avanti Polar Lipids (Alabaster, AL, USA). 1-hexadecanoyl-2-(1-pyrenedecanoyl)-*sn*-Glycero-3-phosphoglycerol ammonium salt (β-py-C_{10}-PG) (PPDPG) was purchased from Invitrogen (Barcelona, Spain). Isopropyl-1-thio-ß-D-galactopyranoside (IPTG) was obtained from Ecogen (Barcelona, Spain), and Bio-Beads SM-2 were purchased from Bio-Rad (Hercules, CA, USA). All other common chemicals were ACS grade.

Bacterial strains and protein purification

E. coli T-184 cells [$lacI^+O^+Z^-(A)$, *rpsL, met, thr, recA, hsdN, hsdR/F,* $lacI^qO^+Z^{D118}$ (Y^+A^+)], and plasmids were kindly provided by Dr. H. Ronald Kaback from the HHMI-UCLA. Mutant (T320W), containing a single-Trp replacement for Thr320, was generated by Dr. J.L. Vázquez-Ibar via two-step PCR [23], and then subcloned as PstI/SpeI fragments into parental Trp-less LacY containing six continuous His residues in the C-terminus, thereby generating Trp-less LacY/T320W. The mutant was sequenced using the dideoxynucleotide method [24]. LacY was extracted and purified from the overproducing strain *E.coli* T-184, according to procedures previously described [6,21 and references thereafter).

Vesicle preparation and protein reconstitution

Liposomes and proteoliposomes were prepared according to methods previously published by our laboratory [6,21,25]. Briefly, chloroform/methanol (3:1, v/v) solutions containing the appropriate amounts of POPE, POPG, and PPDPG were dried under a stream of oxygen-free N_2 in a conical tube. The total concentration of phospholipids was 100 μM. The resulting thin film was kept under high vacuum for approximately 3 hr to remove organic solvent traces. Multilamellar liposomes (MLVs) were obtained following redispersion of the film in 100 mM KH_2PO_4/K_2HPO_4 buffer, pH 7.40, applying successive cycles of freezing and thawing below and above the phase transition of the phospholipids, and sonication for 2 min in a bath sonicator. Afterwards, large unilamellar liposomes (LUVs) supplemented with 0.2% of DDM, to solubilize the lipids, were incubated overnight at room temperature. Liposomes were subsequently mixed with the solubilized protein and incubated at 4 °C for 30 min with gentle agitation, to obtain a lipid-to-protein ratio (LPR) (w/w) of 40. Extraction of DDM was achieved by addition of polystyrene beads (Bio-Beads SM-2, Bio-Rad).

Supported planar bilayer formation and AFM observations

Experiments were carried out as previously described [6,21,25]. All images were recorded in tapping mode with a commercial Digital Instruments (Santa Barbara, CA) Nanoscope III AFM fitted with a 15 μm scanner (d-scanner). Standard Si_3N_4 tips, with a nominal force constant of 0.08 N/m (Olympus, Manheim, Germany), were used and the forces minimized during the scans. Before every sample, the AFM liquid cell was washed with ethanol and ultra

[1] The one-letter amino acid code is used.

pure water (Milli Q reverse osmosis system), and then allowed to dry under an N_2 stream. Mica discs (green mica) were cleaved with scotch and glued onto a Teflon disc by a water-insoluble epoxy. These Teflon discs were glued onto a steel disc and then mounted onto the piezoelectric scanner. All images were scanned under aqueous solution in tapping-mode. Previous to imaging the sample, the tip was stabilized in imaging buffer (10 mM Hepes pH 7.40, 150 mM NaCl, $I = 0.15$ m). Subsequently, 50 μL of liposome samples were pipetted onto freshly cleaved mica. After allowing the vesicles to adsorb at room temperature for 20 min, the surface was gently washed with Ca^{2+} free buffer and the tip immediately immersed in the buffer. Force plots were recorded for every sample to control the repulsion of the tip, and images were flattened using the Nanoscope III program.

Differential scanning calorimetry

DSC analyses were performed using a MicroCal MC-2 calorimeter following previously described procedures [26, 27]. The resulting data were analyzed using the original calorimeter software. The transition temperature (T_m) was taken as the temperature of maximum excess specific heat (and measured to the nearest 0.5°C). Transition enthalpy and cooperativity were calculated according to previously described methods [28]. The calorimetry accuracy for T_m and for enthalpy was ± 0.1°C, and ± 0.2 kcal mol^{-1}, respectively. Each sample was scanned in triplicate over the temperature range 4–40°C at a scan rate of 0.47°C min^{-1}. The base line was horizontal over the temperature range employed.

Fluorescence measurements

Steady state fluorescence measurements were carried out with an SLM-Aminco 8100 (Urbana, IL, USA) spectrofluorometer. The spectrofluorometer's cuvette holder was thermostated with a circulating bath. The excitation and emission bandwidths were 4/4 and 8/8 nm, respectively. Annular and bulk fluidity were determined according to previously described procedures [29]. Pyrene fluorescence was excited at 338 nm, with fluorescence spectra scanned from 350 to 500 nm. For energy transfer measurements, Trp was excited at 292 nm, and the spectra recorded from 300 to 500 nm. In calculating the excimer to monomer fluorescence ratio, we used signal intensities at 378 nm (corresponding to the peak of monomer band) and 470 nm (maximum of pyrene excimer band).

Based on the quenching of intrinsic tryptophan by pyrene phospholipids, the values of energy-transfer efficiency (ET) were determined according to the equation

$$ET = 1 - I/I_0 \quad (1)$$

where I_0 and I are the tryptophan emission intensities in the absence or presence of pyrene phospholipid derivative, respectively [30]. The intensities were evaluated from de peak height of the 338 nm tryptophan fluorescence under excitation at 292 nm

Results and discussion

Calorimetric determinations of 3:1 POPE:POPG liposomes yielded transition curves as shown in Fig. 2. In the temperature interval studied, only one transition appeared. The temperature of maximal excess specific heat (T_m) occurred at 20.90 ± 0.30°C (mean ± SD, $n = 3$). The width at the half-height of the thermogram was 4.68 ± 0.20°C (mean ± SD, $n = 3$). Interestingly, the heat capacity curve was skewed towards low temperatures. The enthalpy change of the endotherm was 19.62 ± 0.2 kJ·mol^{-1} (mean ± SD, $n = 3$)[2].While neither microdomains nor phase separations have been observed in 3:1 POPE:POPG bilayers (viewed via solid-state NMR at 30 °C) [31], the pronounced tailing at the low temperature side of the heat capacity curve suggests that POPE and POPG rich microdomains do exist [32]. Using AFM we have reported in a previous work [21], the existence of two laterally segregated domains in supported planar bilayers (SPBs) formed from liposomes of 3:1 POPE:POPG. In the bottom of Fig. 2, of the present work, the AFM topography images show both domains (distinguisible by differences in the coloration) responded to temperature changes. The thickness of the bilayers, calculated by measuring the difference between the lipid and the substrate (mica), were consistent with values previously reported [21]. The interdomain difference 0.52 ± 0.01 nm was almost unaffected by increasing the temperature. Taking the total area covered by the SPB in each image as the 100% (bottom Fig. 2), it has been calculated that the upper domain increased from 30 to 34% of the total area with a concomitant decrease in the area of the lower domain. Having into account that the area fraction covered by the upper domain matches approximately with the nominal composition of the liposome preparation, it is reasonable to assume that the upper domain observed in Fig. 2 (bottom) corresponded to POPG-enriched areas.

Typically, the excited-state pyrene molecules display two characteristic peaks in the fluorescence spectra: monomer (M) and excimer (E), respectively. The specific E/M ratio depends on the collision rate of the pyrene molecules [20 and references thereafter]. When the pyrene molecule was excited at its own wavelength of 338 nm, the E/M ratios provided the bulk fluidity (lateral diffusion). Figure 3 shows

[2] The value for the POPE:POPG containing $X_{PPDPG} = 0.01$ was $T_m = 18.19$°C; the width at half-height of the thermogram 7.81°C; and the enthalpy change of the endotherm measured 13.90 kJ·mol^{-1}.

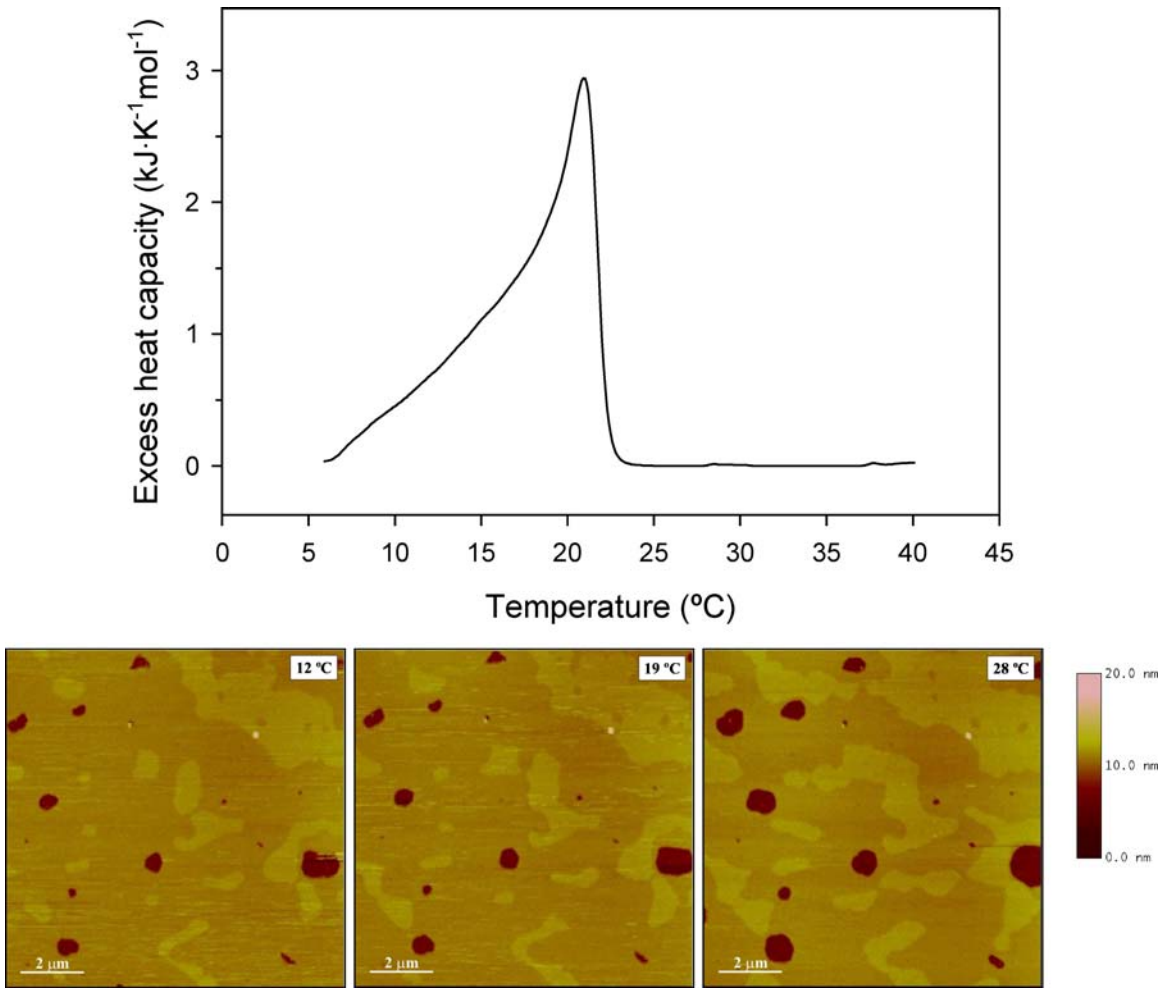

Fig. 2 Excess heat capacity measured as a function of temperature for POPE:POPG. (3:1, mol/mol) multilamellar liposomes. Bottom: Topography images obtained from the extension of POPE:POPG (3:1, mol/mol) liposomes by AFM. Images were obtained in tapping mode using as an imaging buffer 10 mm Hepes pH 7.40, 150 mM NaCl, 20 mM CaCl2, I = 0.19 m

the *E*/*M* ratios of PPDPG in LUVs and proteoliposomes under increasing temperatures. For liposomes, *E*/*M* ratio values decreased until 20°C, which was approx. the T_m of the POPG:POPE mixture, following a moderate increase until 38°C. The decrease in the PPDPG excimers formation could be attributed to the relative increase in the area of the upper domain. Consequently, collision between monomers and excimer formation will occur less frequently. We suggest that the changes in the fraction area covered by each domain should lead to a redistribution of PPDPG molecules in the bilayer, thereby explaining the observed decrease of the *E*/*M* ratio. When LacY was incorporated into liposomes, relative decreases in excimer formations by the fluorescent probe resulted across all temperature ranges when pyrene was excited. Similar behavior has been observed following the addition of the amyloid-β-peptide to rat synaptic plasma membranes [29]. Clearly, LacY promotes the separation of the probe molecules. There is no contradiction between this observation and similar experiments previously reported [20]. Nor is it difficult to reconcile both observations taking into account the fact that we are using: (i) a 3:1 POPE:POPG mixture instead of POPG; and (ii) a lower lipid-to-protein ratio. Importantly, the correct structure and function of the permease has been shown to be optimal at a LPR $\approx$ 12 [15]. Moreover, our choice of LPR was identical to that used in a previously published paper [21]. In fact, we have confirmed that the presence of lactose permease decreases the ratio *E*/*M* ratio in a manner that can be related to the LPR (data not shown).

The emission spectrum of intrinsic tryptophan from the mutant T320W overlaps with the absorption spectrum of the PPDPG phospholipid derivative. Accordingly, in the model shown in Fig. 1, the residue 320 (located at the protein–lipid boundary) is interacting with the phospholipid acyl chains. Thus, only those PPDPG molecules surrounding the protein, termed annular lipids, will be selectively excited. Consequently, the *E*/*M* ratio provides the necessary information on the fluidity for the annular lipids. Figure 4 shows the excimer

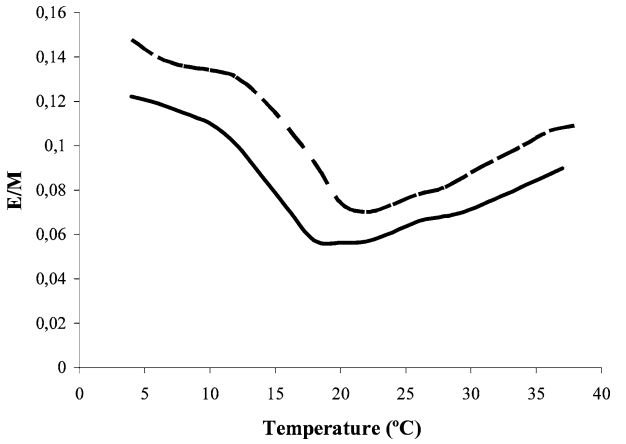

Fig. 3 Excimer and monomer intensities fluorescence ratio (E/M) for liposomes (– – –) and proteoliposomes (—). Pyrene was exited at 338 nm at different temperatures. This experiment was repeated six times with essentially identical results

and monomer intensities, as well as the E/M ratio versus temperature curves, obtained for POPE:POPG:PPDPG in 3:0.99:0.1 molar ratio, proteoliposomes.

As shown in Fig. 4C, the *E*/*M* ratios decreases until the T_m of the 3:1 POPE:POPG mixture, following a slow increase up to 38°C, which is similar to what was described in Fig. 3 for bulk lipids. Remarkably, the *E*/*M* ratios were always higher for the annular region than for the bulk phase, indicating: (i) a higher fluidity for annular lipids, in comparison with bulk lipids and (ii) the presence of excimers immediately surrounding the protein.

Values for excimer intensities (Fig. 4A) changed in reciprocal fashion to those obtained for monomer intensities (Fig. 4B) until the gel-to-liquid phase transition of the phospholipid mixture was attained. When $T < T_m$, the excimer intensity sharply decreased while the monomer intensity slightly increased (Fig. 4A and 4B, respectively), thus indicating an increase in the lateral diffusion of the bilayer pyrene lipid molecules. Any further increase in temperature resulted in an almost constant excimer intensity value, as well as a continuous decrease in monomer intensity.

The tryptophan fluorescence quenching caused by pyrene (Fig. 5) indicated that tryptophan and pyrene are separated during the gel phase into the bilayer with the minimum value reached at ≈ 8°C. Subsequently, progressive increases in ET values were observed until the T_m (see the corresponding the minimum value in the *E*/*M* representation, Fig. 4C). Further increases in temperature only caused a slight increase in ET. Our results are in agreement with recent findings on the requirement of anionic phospholipids at the interfacial lipid binding site of a potassium channel [33].

The results presented in this paper underscore the fact that PG, present in the annular region, may transfer protons via hydrogen bonds to certain amino acids involved in the translocation mechanism. It is well known that PE

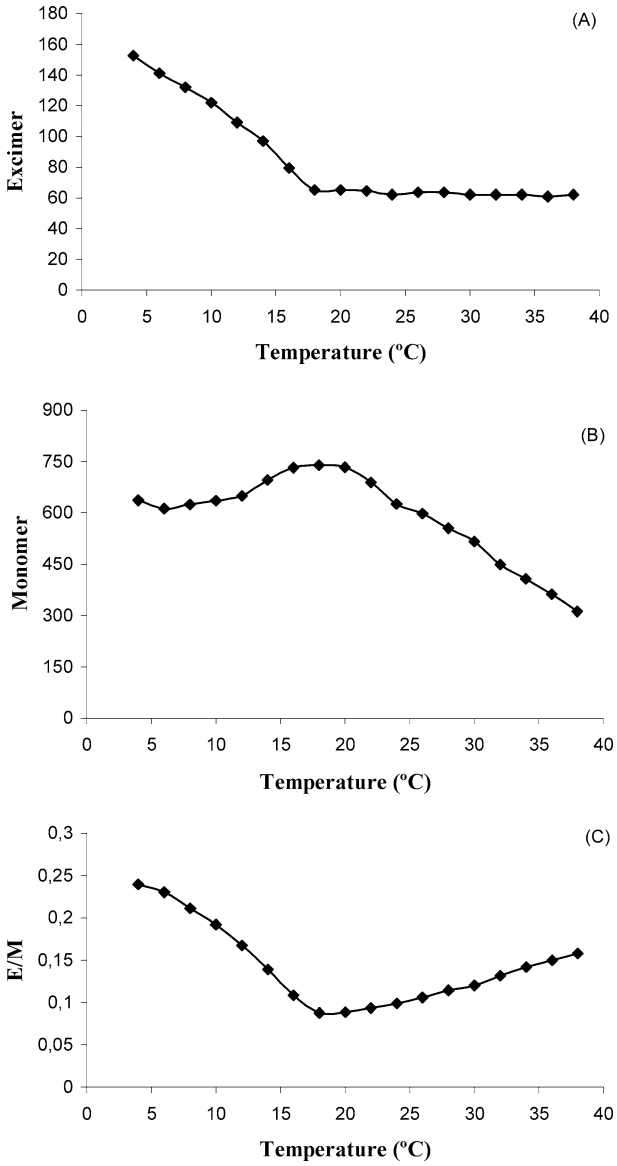

Fig. 4 Excimer (A), monomer (B), and excimer/monomer (E/M) (C) intensities versus temperature curves obtained for POPE:POPG liposomes containing a 0.01 molar fraction of PPDPG. Pyrene was excited at 292 nm. This experiment was repeated six times with essentially identical results

may establish intermolecular hydrogen bonding to an even greater extent than PG. Therefore, similar experiments to those described in the present paper, employing an adequate PE pyrene derivative, should be conducted. This work is currently underway in our laboratory.

Acknowledgments L. P. is the recipient of a collaborative fellowship from the Ministerio de Educación y Ciencia, and a S. M-M. is a fellow of 'Recerca i Docència' from the Universitat de Barcelona. We would like to thank Professor Ronald Kaback for the materials provided, and Dr. José Luis Vázquez-Ibar for engineering the single-Trp mutant, as well as for helpful comments on the original manuscript. This work was supported by grants CTQ 2005-07989 from the Ministerio de Educación y Ciencia, Spain.

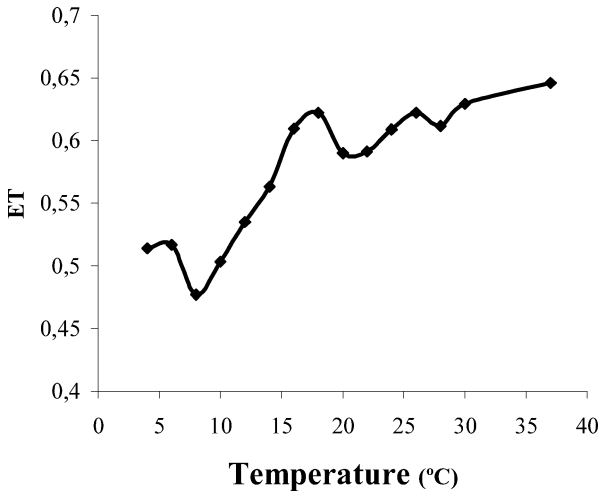

Fig. 5 Energy transfer efficiency from intrinsic tryptophan to pyrene phospholipid derivative in POPE:POPG proteoliposomes

References

1. Venkatessen P, Kaback HR (1998) The substrate-binding site in the lactose permease of *Escherichia coli*. Proc Natl Acad Sci U.S.A. 95:165–184
2. Kaback HR, Wu J (1999) What to do while awaiting crystals of a membrane transport protein and thereafter. Acc Chem 32:805–813
3. Abramson J, Smirnova I, Kasho V, Verner G, Kaback HR, Iwata S (2003) Structure and mechanism of the lactose permease of *Escherichia coli*. Science 301:610–615
4. Martz E (2002) Protein Explorer: easy yet powerful macromolecular visualization. TIBS 27:107–109
5. Lee AG (2003) Lipid–protein interactions in biological membranes: a structural perspective. Biochim Biophys Acta, 1612:1–40
6. Merino S, Domènech Ò, Montero MT, Hernández-Borrell J (2005) Atomic force microscopy study of *Escherichia coli* lactose permease proteolipid sheets. Biosens Bioelectr 20:1843–1846
7. Zhuang J, Privé GG, Werner GE, Ringler P, Kaback HR, Engel A (1999) Two dimensional crystallization of *Escherichia coli* lactose permease. J Struct Biol 125:63–75
8. Merino-Montero S, Domènech Ò, Montero MT, Hernandez-Borrell J (2005) Preliminary atomic force microscopy study of two-dimensional crystals of lactose permease from *Escherichia coli*. Biophys Chem 118: 114–119
9. Viitanen P, Newman MJ, Foster DL, Wilson TH, Kaback HR (1986) Purification, reconstitution, and characterization of the lac permease of *Escherichia coli*. Methods Enzymol 125:429–452
10. Jung K, Jung H, Wu J, Privé GG, Kaback HR (1993) Use of site-directed fluorescence labeling to study proximity relationships in the lactose permease of *Escherichia coli*. Biochemistry 32:12273–12278
11. Jung K, Jung H, Kaback HR (1994) Dynamics of lactose permease of *Escherichia coli* determined by site-directed fluorescence labeling. Biochemistry 33:3980–3985
12. Offenbacher H, Wolfbeis OS, Fürliger E (1986) Fluorescence optical sensors for continuous determination of near neutral pH values. Sens Actuat 9:73–84
13. Kiefer H, Klee B, John E, Stierhof YD, Jähnig F (1991) Biosensors based on membrane transport proteins, Biosensors Biolectron 6:233–237
14. Klee B, John E, Jähnig F (1992) Biosensor based on the membrane protein lactose permease. Sens Actuat B 7:376–379
15. Le Coutre J, Narasimhan LR, Patel CKN, Kaback HR (1997) The lipid bilayer determines helical tilt angle and function in lactose permease of *Escherichia coli*. Proc Natl Acad Sci U.S.A. 94:10167–10171
16. Vázquez-Ibar JL, Weinglass AB, Kaback HR (2002) Engineering a terbium-binding site into an integral membrane protein for luminescence energy transfer. Proc Natl Acad Sci U.S.A. 99:3487–3492
17. Zhao M, Zen KC, Hubbell WL, Kaback HR (1999) Proximity between Glu126 and Arg144 in the Lactose Permease of *Escherichia coli*. Biochemistry 38:7407–7412
18. Bogdanov M, Dowhan W (1995) Phosphatidylethanolamine is required for *in vivo* function of the membrane-associated lactose permease of *Escherichia coli*. Biol Chem 270:732–739
19. Bogdanov M, Sun J, Kaback HR, Dowhan W (1996) A Phospholipid Acts as a Chaperone in Assembly of a Membrane Transport Protein. J Biol Chem 271:11615–11618
20. Lehtonen JYA, Kinunen PKJ (1997) Evidence for phospholipids microdomain formation in liquid crystalline liposomes reconstituted with *Escherichia coli* lactose permease. Biophys J 72:1247–1257
21. Merino S, Domènech Ò, Montero MT, Hernández-Borrell J (2005) Effects of lactose permease on the phospholipid environment in which it is reconstituted: A fluorescence and atomic force microscopy study. Langmuir 21:4642–4647
22. Houslay MD, Stanley KK (1982) Dynamics of Biological Membranes. Influence on synthesis, structure and function. Wiley, New York
23. Jung K, Jung H, Colacurcio P, Kaback HR (1995) Role of glycine residues in the structure and function of lactose permease, an *Escherichia coli* membrane transport protein. Biochemistry 34:1030–1039
24. Sanger F, Nicklen S, Coulsen AR (1977) DNA Sequencing with Chain-Terminating Inhibitors. Proc Natl Acad Sci U.S.A. 74:5463–5467
25. Merino S, Domènech Ò, Díez-Perez I, Sanz F, Montero MT, Hernández-Borrell J (2005) Surface thermodynamic properties of monolayers versus reconstitution of a membrane protein in solid supported bilayers. Colloids Surf B:Biointerfaces 44, 93–98
26. Villaverde J, Cladera J, Hartog A, Berden J, Padrós E, Duñach M (1998) Nucleotide and Mg^{2+} dependency of the thermal denaturation of mitochondrial F_1-ATPase. Biophys J 75:1980–1988
27. Villaverde J, Cladera J, Padrós E, Rigaud JL, Duñach M (1997) Effect of nucleotides on the thermal stability and on the deuteration kinetics of the thermophilic F_0F_1 ATP synthase. Eur J Biochem 244:441–448
28. Tilcock CPS, Fisher D (1979) Interaction of phospholipid membranes with poly(ethylene glycol)s. Biochim Biophys Acta 577:53–61
29. Mason RP, Jacob RF, Walter MF, Mason PE, Avdulov NA, Chochina SV, Igbavboa U, Wood WG (1999) Distribution and fluidizing action of soluble and aggregated amyloid- β-peptide in rat synaptic plasma membranes. J Biol Chem 274:18801–18807
30. Lakowicz JR (1999) Principles of Fluorescence Spectroscopy, 2nd edn. Kluwer Academic/Plenum, New York
31. Hallock KJ, Lee DK, Omnaas J, Mosberg HI, Ramamoorthy A (2002) Membrane composition determines pardaxin's mechanism of lipid bilayer disruption. Biophys J 83:1004–1013
32. Lohner K, Latal A, Degovics G, Garidel P (2001) Packing characteristics of a model system mimicking cytoplasmic bacterial membrane. Chem Phys Lipids 111:177–192
33. Marius P, Alvis SJ, East JM, Lee AG (2005) The interfacial lipid binding site on the potassium channel KcsA is specific for anionic phospholipids. Biophys J 89:4081–4089